Living with a Star Targeted Research and Technology

Flare Dynamics in the Lower Solar Atmosphere

Annual Team Progress Report

February 2015 to February 2016

Joel Allred (NASA GSFC): Team 1

Phil Judge (High Altitude Observatory, Lucia Kleint PI until Sept. 2014): Team 2

Alexander Kosovichev (New Jersey Institute of Technology): Team 3

Chang Liu (New Jersey Institute of Technology): Team 4

Vahe Petrosian (Stanford University): Team 5

Haimin Wang (New Jersey Institute of Technology, Team Leader): Team 6

This is the third year of the LWS Focused Science Team (FST). Our collaborative efforts have continued to focus on the following three objectives: (1) understanding the transport of energy and momentum into the interior from the solar atmosphere during flares, (2) understanding high-energy phenomena in the impulsive phase of flares, especially the transport of high-energy particles from the corona in relation to the thick-target model, and (3) studying the changes of vector magnetic fields in the photosphere associated with flares. We had three team meetings in 2015 and published 24 journal papers. In this report, we summarize the progress in the aspects of organization of the team effort, highlights of scientific achievements, and the tasks for the year 4.

1. Organization of Team Effort

In the past year, we organized three team meetings. The first meeting was held at NJIT, in connection with 14th RHESSI workshop, August 12-15, 2015. Much of our team effort is very relevant to general sciences goals of RHESSI, we benefited significant in sharing our research results with the entire RHESSI team. The second meeting is via WebEx, on Sept. 23, 2015. Besides science presentations, we discussed the preparation of the 3rd year review. The final meeting was held in Stanford University on December 13, 2015. It also served as our 3rd year review. Each team summarized the results of 3 years, and related collaborative efforts. The team generated a power point file that was presented in the LWS Town Hall meeting on December 14, 2015 in San Francisco.

2. Progress in Collaborative Projects

This focus team has been very active in our collaborating efforts, including the common science interests, the analysis of team events and comparison between observations and modeling. Here we give some key collaborative effort.

Teams 2 and 5 used RADYN simulations that match very well with observations of spectral line profiles.
Teams 2, 4, 6 carried out IRIS and magnetic field data analysis, discovered new flare topologies and emission patterns.
Teams 1 and 6 collaborated on the discovery and understanding of negative flares.
Teams 3 and 5 collaborated on thick-target modeling.
Teams 3, 4, 6 collaborated on analysis and gained basic understanding of sunquakes.
Teams 1 and 5 combined Stanford flare code with hydrodynamic code successfully.

3. Highlights of Scientific Achievements

3.1. Understanding the transport of energy and momentum into the interior from the solar atmosphere during flares

Kosovichev team studied the M9.3 solar flare on 2011 July 30 that produced a “sunquake,” In addition to the helioseismic waves, the flare caused a large expanding area of white-light emission and was accompanied by the rapid formation of a sunspot structure in the flare region.

The flare produced hard X-ray (HXR) emission less than 300 keV and no coronal mass ejection (CME). The absence of CME rules out magnetic rope eruption as a mechanism of helioseismic waves. The sunquake impact does not coincide with the strongest HXR source, which contradicts the standard beam-driven mechanism of sunquake generation (Sharykin et al., 2015a).

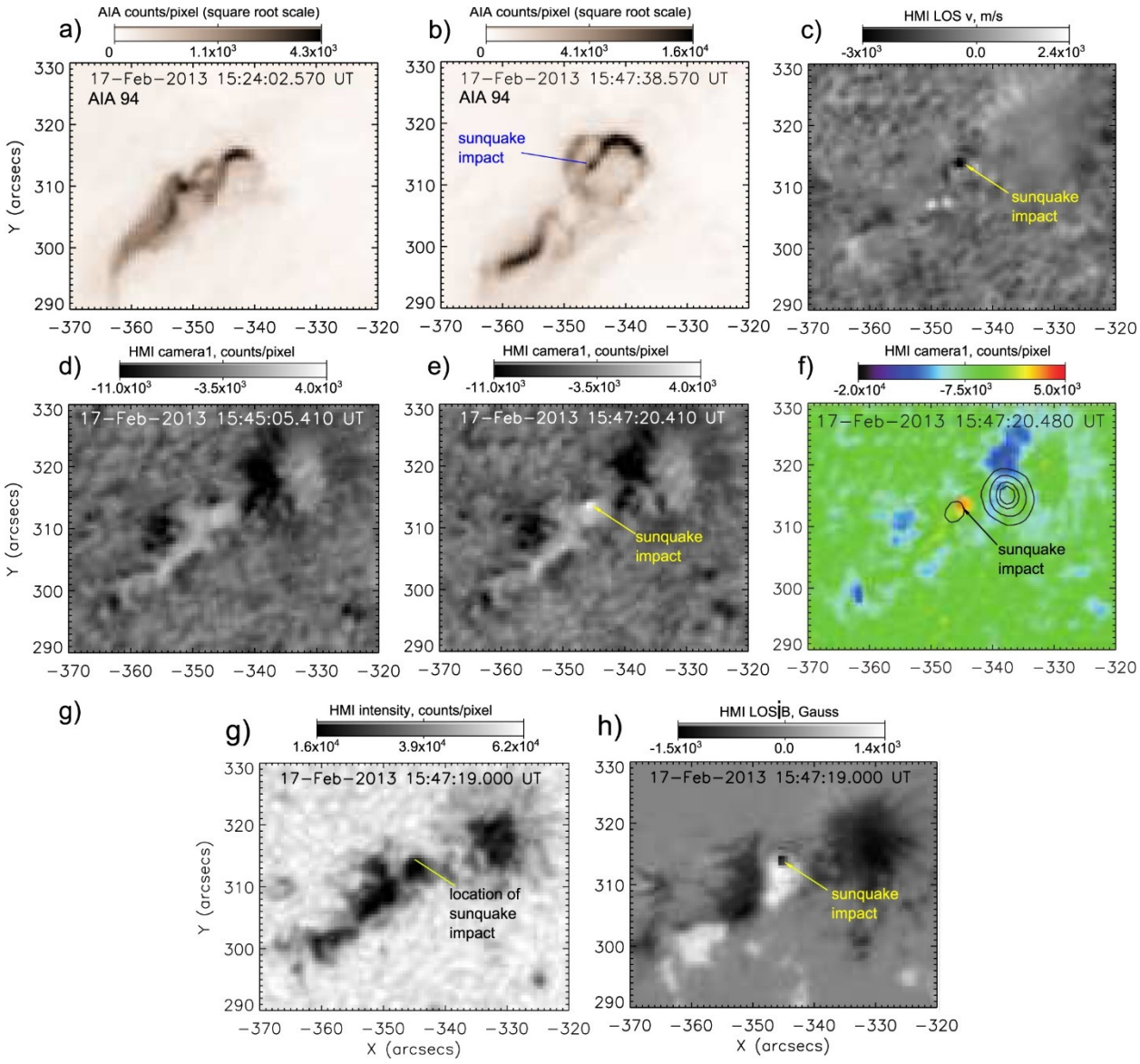

Figure 1. Location of the sunquake initial impact associated with C7.0 class flare. AIA 94 Å images: (a) before and (b) during the flare; (c) line-of-sight Dopplergram showing the impact location; time differences: (d) before and (e) during flare of the HMI level-1 filtergram; (f) comparison with RHESSI 50–100 keV intensity contours (40%, 60%, 80%, and 90%); (g) HMI intensity and (h) line-of-sight magnetogram showing the impact location (Sharykin et al., 2015a).

Allred et al. (2015) presented a unified computational framework that can be used to describe impulsive flares on the Sun and on dMe stars. The models assume that the flare impulsive phase is caused by a beam of charged particles that is accelerated in the corona and propagates downward depositing energy and momentum along the way. This rapidly heats the lower stellar atmosphere causing it to explosively expand and dramatically brighten. The models consist of flux tubes that extend from the sub-photosphere into the corona. They simulated how flare-accelerated charged particles propagate down one-dimensional flux tubes and heat the stellar atmosphere using the Fokker–Planck kinetic theory. Detailed radiative transfer is included so that model predictions can be directly compared with observations. The flux of flare-accelerated particles drives return currents which additionally heat the stellar atmosphere. These effects are also included in our models. They examined the impact of the flare-accelerated particle beams on model solar and dMe stellar atmospheres and perform parameter studies varying the injected particle energy spectra. The found the atmospheric response is strongly dependent on the accelerated particle cutoff energy and spectral index. Figure 2 shows the example of the modeling.

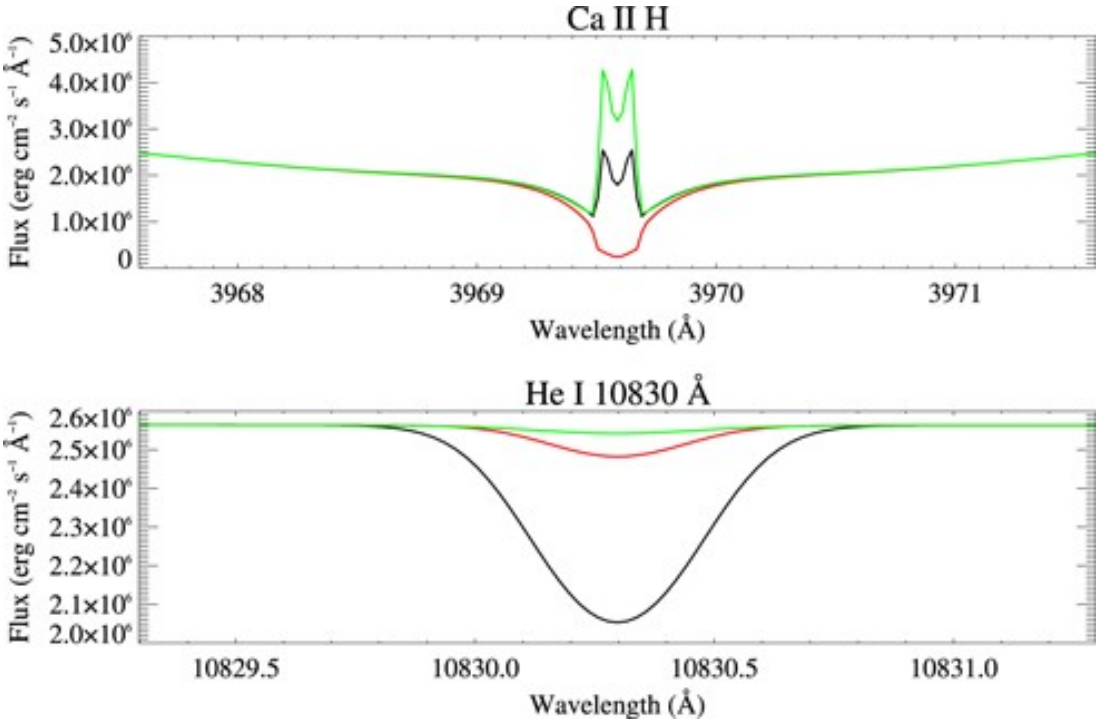

Figure 2. Profiles for the Ca II H and He I 10830 A lines from the loop models generated using XEUV backwarming (black), the technique of previous study by the author (green), and without XEUV backwarming (red) (Allred et al., 2015).

Kosovichev team analyzed the C7.0 solar flare of 2013, February 17, revealed a strong helioseismic response (sunquake) caused by a compact impact observed with the Helioseismic and Magnetic Imager (HMI) on board SDO in the low atmosphere. This is the weakest known C-

class flare generating a sunquake event. It is found that the photospheric flare impact does not spatially correspond to the strongest hard X-ray emission source, but both of these events are parts of the same energy release. Their analysis reveals a close association of the flare energy release with a rapid increase in the electric currents and suggests that the sunquake initiation is unlikely to be caused by the impact of high-energy electrons, but may be associated with rapid current dissipation or a localized impulsive Lorentz force in the lower layers of the solar atmosphere (Sharykin et al., 2015b).

Liu et al. (2015) revealed that active filament flux ropes can reside within a dome-shaped magnetic field structure consisting of a central region encompassed by opposite-polarity regions. The filament can become unstable and rise upward due to MHD instability, interacting with the fan-spine-like magnetic fields. This would lead to a partial opening of the dome and a circular-ribbon flare. Importantly, the sunquake sources found in the 2014 March 29 circular-ribbon flare are located not at the footpoints (as in the case of the 2011 February 15 X2.2 flare) but at the middle section of the erupting flux rope cospatial with the flare hard X-ray footpoints. As a further comparison, in another circular-ribbon flare on 2012 October 23, the sunquake source is rather extended spanning the entire scale of the erupting flux rope. These observations raise intriguing questions on the relationship between the flux rope eruption and sunquake generation.

3.2 Understanding high-energy phenomena in the impulsive phase of flares

Collaborating with Kleint, Petrosian team used RADYN radiative code treats the H, He, Mg and Ca atoms in non-local thermody- namic equilibrium conditions, allowing them to study their transitions in detail and to compare estimated energy fluxes with spectral observations taken with different instruments at different wavelengths. This code however, requires the input of some energy by accelerated particles. This is usually done by assuming a flux of particles with a power-law spectrum. The combined Stanford-RADYN code provide this input more accurately. In addition, we use RHESSI HXR observations to constrain the spectrum of accelerated electrons and use the accurate transport code to determine the spatial distribution of the energy deposition. Rubio da Costa et al. (2015a) compared the RADYN-predicted intensity and shape of the Halpha and Ca II 8542 A lines with those observed by the Dunn Solar Telescope (DST) IBIS spectro-polarimeter. This is the most self-consistent treatment of this problem attempted so far. They found some interesting results. While the Ca II 8542 A observations are fit adequately, the Halpha observations seem to require the presence of some micro-turbulence.

Petrosian aslo team combined Fokker-Planck particle acceleration and transport code, the Stanford Flare code, with the HD RADYN code that includes detailed radiative transfer calculations. They completed a comprehensive paper describing this major undertaking (Rubio da Costa et al. 2015b). The team generalized the previous work on the inversion of RHESSI counts to obtain the accelerated electron spectra and from them the characteristics of the acceleration mechanisms, to flares with only total spectral information, which are more numerous. These larger available data set will allow a more rigorous tests of the above results. They also used these ideas to resolve the discrepancies between the spectra of hard X-ray emitting and (prompt and delayed) SEP electrons discovered by Krucker et al. (2007, ApJ Letters, 663, L109). A paper describing the results of this work will be submitted to the Astrophysical Journal shortly (Petrosian 2016).

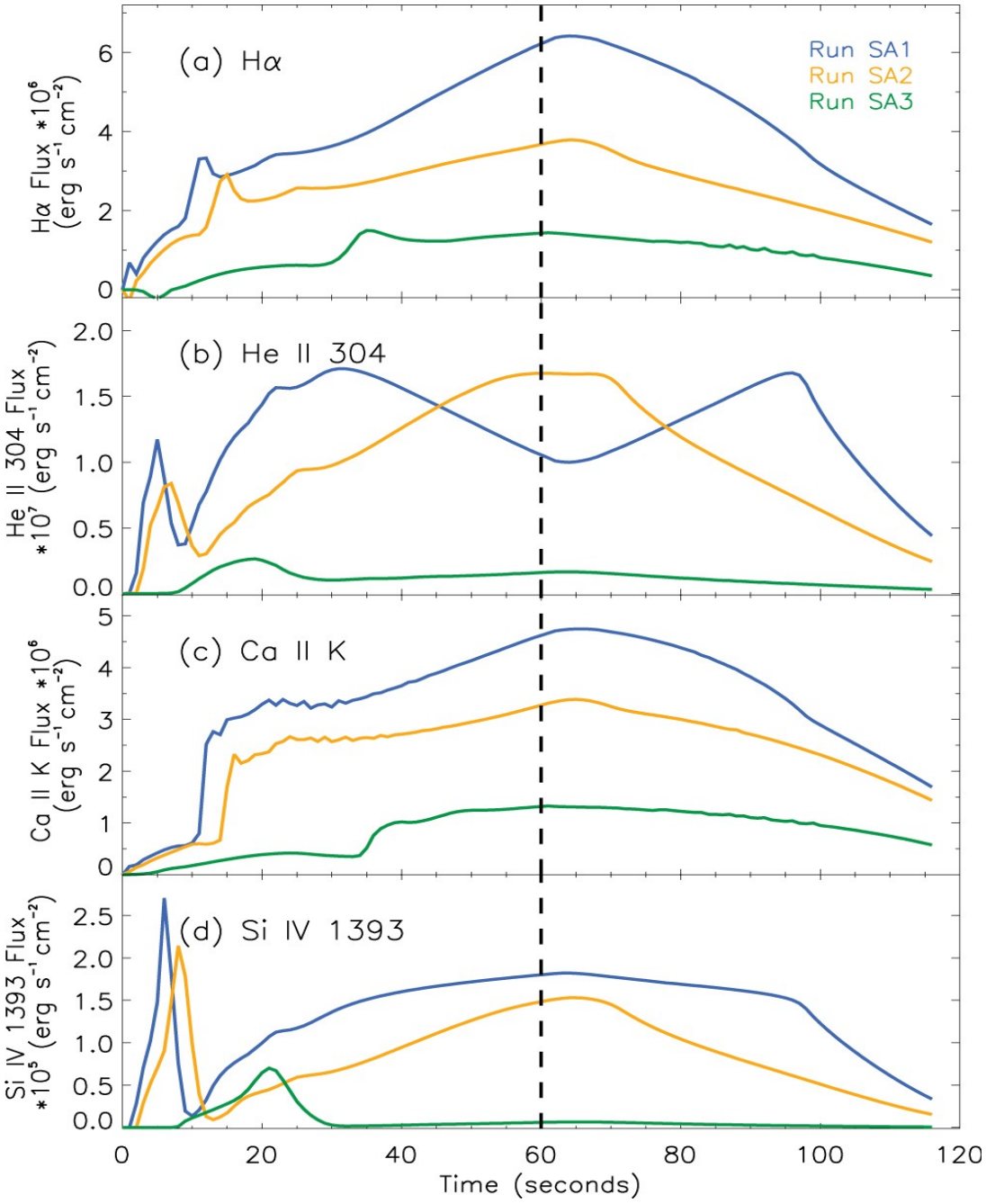

Figure 3. Light curves of the Hα 6563 Å, He II 304 Å, Ca II K 3934 Å, and Si IV 1393 Å lines From the simulation. The emission at the initial time has been subtracted. The vertical dashed line indicates peak time of the flare (Rubio da Costa et al. 2015b).

Kleint et al. (2016) combined observations from IRIS HMI and the ground-based Facility Infrared Spectrometer instrument, covering wavelengths in the far-UV, near-UV (NUV), visible, and infrared during the X1 flare on March 29, 2014. Fits of blackbody spectra to infrared and

visible wavelengths are reasonable, yielding radiation temperatures ~6000–6300 K. The NUV emission, formed in the upper photosphere under undisturbed conditions, exceeds these simple fits during the flare, requiring extra emission from the Balmer continuum in the chromosphere. Thus, the continuum originates from enhanced radiation from photosphere (visible-IR) and chromosphere (NUV). From the standard thick-target flare model, they calculated the energy of the non-thermal electrons observed by RHESSI and compared it to the energy radiated by the continuum emission. They found that the energy contained in most electrons >40 keV, or alternatively, of ~10%–20% of electrons >20 keV is sufficient to explain the extra continuum emission.

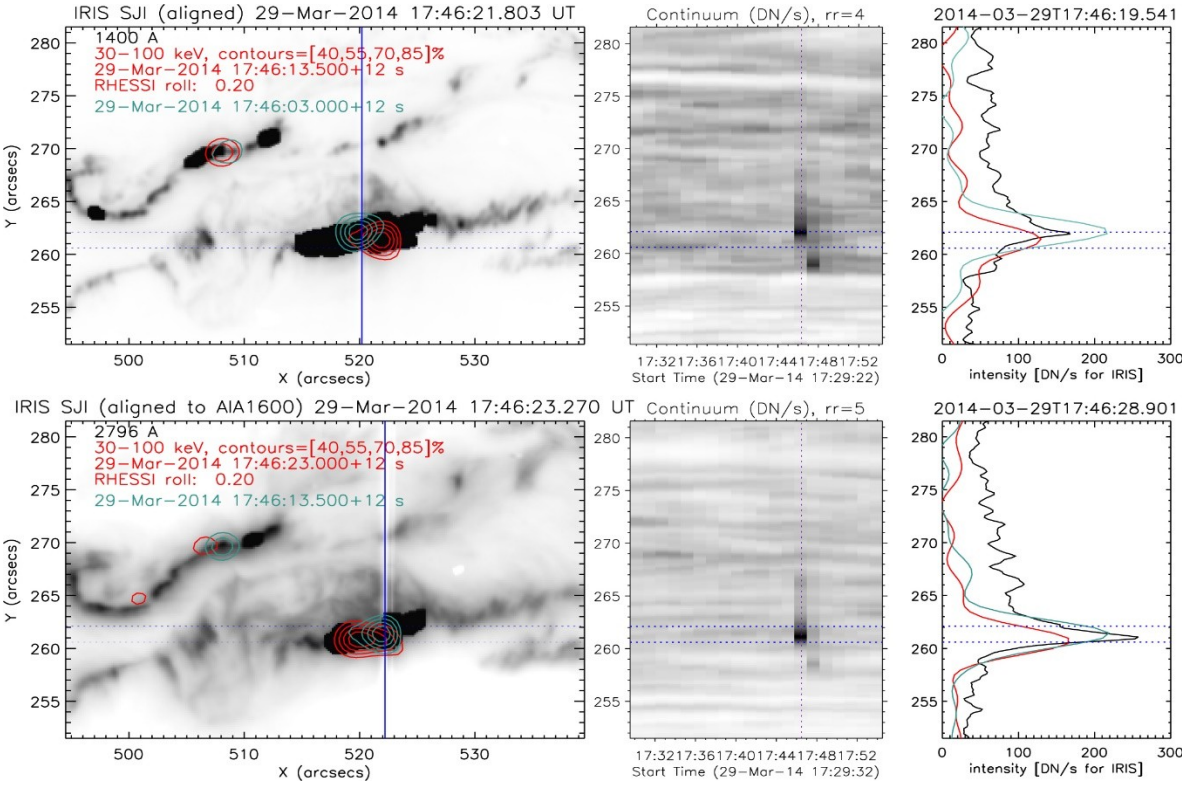

Figure 4. Study of March 29, 2014 X1 flare. Left column: RHESSI contours (red; light blue for 10 s earlier) on color-reversed IRIS SJI with the slit marked blue. Middle column: color-reversed continuum intensity evolution showing the continuum emission in black. The dotted vertical purple line indicates the location where the intensity for the plots in the right column was derived. Right column: intensity cross-section at the given raster step and time (see image titles). The red line (light blue line for 10 s earlier) is the RHESSI intensity cut (in arbitrary units) at the same time and solar X. The maxima of the IRIS continuum and RHESSI HXR emission nearly coincide. The horizontal dashed lines are for reference to indicate the same locations in all three panels (Kleint et al., 2016).

Fleishman et al. (2015) presented detailed 3D modeling of a dense, coronal thick target X-ray flare using the GX Simulator tool, photospheric magnetic measurements, and microwave imaging and spectroscopy data. The developed model offers a remarkable agreement between the synthesized and observed spectra and images in both X-ray and microwave domains, which

validates the entire model. The flaring loop parameters are chosen to reproduce the emission measure, temperature, and the fast electron distribution at low energies derived from the X-ray spectral fit, while the remaining parameters, unconstrained by the X-ray data, are selected such as to match the microwave images and total power spectra. The modeling suggests that the accelerated electrons are trapped in the coronal part of the flaring loop, but away from where the magnetic field is minimal, and, thus, demonstrates that the data are clearly inconsistent with electron magnetic trapping in the weak diffusion regime mediated by the Coulomb collisions. Thus, the modeling supports the interpretation of the coronal thick-target sources as sites of electron acceleration in flares and supplies us with a realistic 3D model with physical parameters of the acceleration region and flaring loop.

3.3 Studying the changes of vector magnetic fields in the photosphere associated with flares

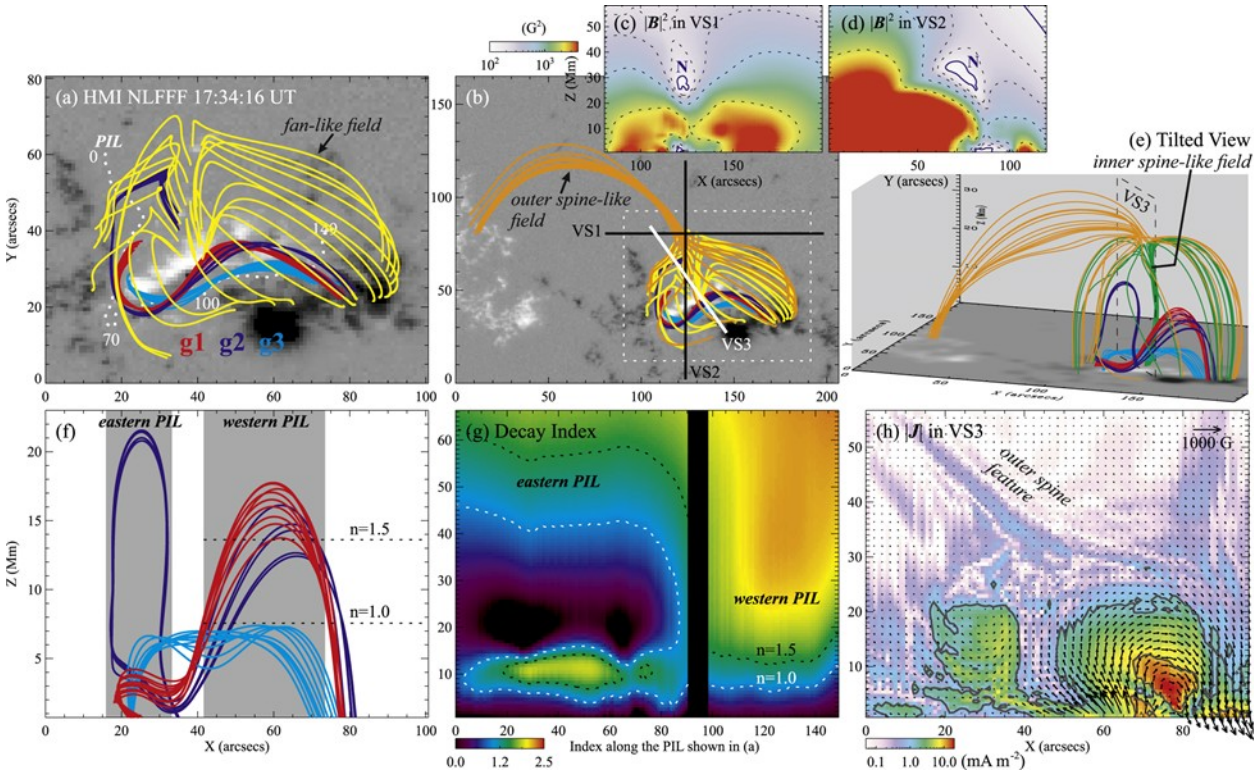

Figure 5. Magnetic field structure of March 29, 2014 flare. (a), (b), and (e) Selected NLFFF lines computed based on remapped HMI magnetogram, illustrating FRs g1–g3 and the quasi-fan-spine fields. (c) and (d) distribution in the vertical slices VS1 and VS2 (bottom sides marked in (b)).. (f) A side view of FRs. (g) Spatial distribution of decay index along the PIL as plotted in (a). (h) distribution over the vertical slice VS3 (denoted in (b) and (e)), overplotted with projected field vectors (Liu et al., 2015).

Liu et al. (2015) analyzed the GOES-class X1.0 flare on 2014 March 29 8), in which they found an asymmetric eruption of a sigmoidal filament and an ensuing circular flare ribbon. Initially both EUV images and a preflare nonlinear force-free field model show that the filament is embedded in magnetic fields with a fan-spine-like structure. In the first phase, which is defined

by a weak but still increasing X-ray emission, the western portion of the sigmoidal filament arches upward and then remains quasi-static for about five minutes. The western fan-like and the outer spine-like fields display an ascending motion, and several associated ribbons begin to brighten. Also found is a bright EUV flow that streams down along the eastern fan-like field. In the second phase that includes the main peak of hard X-ray (HXR) emission, the filament erupts, leaving behind two major HXR sources formed around its central dip portion and a circular ribbon brightened sequentially. The expanding western fan-like field interacts intensively with the outer spine-like field, as clearly seen in running difference EUV images. They discussed these observations in favor of a scenario where the asymmetric eruption of the sigmoidal filament is initiated due to an MHD instability and further facilitated by reconnection at a quasi-null in corona; the latter is in turn enhanced by the filament eruption and subsequently produces the circular flare ribbon. See Figure 5 above.

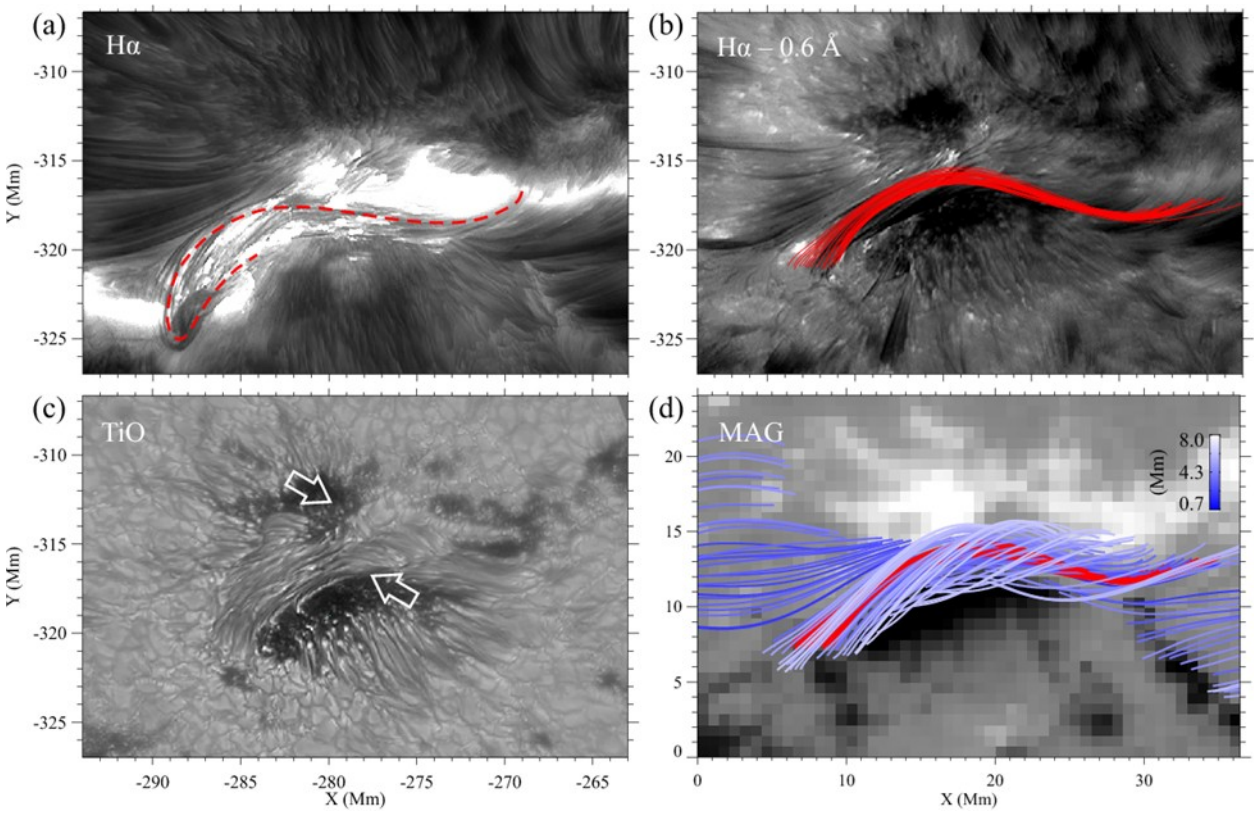

Figure 6. Fine details of a magnetic flux rope captured by the New Solar Telescope at Big Bear Solar Observatory for Solar Active Region 11817 on 2013 August 11. The structure is further demonstrated by the 3-D magnetic modeling based the observations of HMI (Wang et al., 2015).

Wang et al. (2015) presented observations of a flaring using the highest resolution chromospheric images from the 1.6-m New Solar Telescope at Big Bear Solar Observatory, supplemented by a magnetic field extrapolation model. A set of loops initially appear to peel off from an overall

inverse S-shaped flux bundle, and then develop into a multi-stranded twisted flux rope, producing a two-ribbon flare. We show evidence that the flux rope is embedded in sheared arcades and becomes unstable following the enhancement of its twists. The subsequent motion of the flux rope is confined due to the strong strapping effect of the overlying field. These results provide a first opportunity to witness the detailed structure and evolution of flux ropes in the low solar atmosphere (see Figure 6).

4. Focus of Research in 2016

Our data analysis and modeling efforts have achieved significant results for two X-class flares: (1) 2011 February 15, (2) 2014 March 29. In the final year, we will concentrate on 2 other team events, (3) 2014 October 24 and (4) 2015 June 22. All the events have comprehensive coverage in the RHESSI HXR, make the modeling comparison feasible. For event (3), the data review and some initial ideas were discussed in December 2014 team meeting. Hinode, NSO, IRIS all had good observational coverage. Event (4) was discussed in detail in December 2015 team meeting.

Observation and Data Analysis:

- Investigate the statistical relationship between the sunquake sources detected by the time-distance and holography techniques. Investigate magnetic field and continuum emission variations in sunquake events, and also the relationship between these variations and high-energy flare emissions.

-Investigate magnetic field and continuum emission variations in sunquake events, and also the relationship between these variations and high-energy flare emissions.

- Continue spectro-polarimetric analysis of flares obtained with BBSO/NST and NSO/IBIS.
-IRIS, microwave, and hard X-ray data will be jointly analyzed.

- Study the evolution of vector magnetic fields and velocity fields associated with flares. NLFFF extrapolation tools will be utilized to understand the 3D field restructuring. The 2014 October 24 and 2015 June 22 events will be emphasized.

Modeling:

-Continue exploration of the acceleration mechanism of electrons and start on expanding the acceleration-transport code to include acceleration of protons.

-Perform realistic 3D simulations of the atmospheric and helioseismic responses to solar flares.
-Data Driven MHD simulation to trace the magnetic structure of eruptions.

Meetings:

Two team meetings will be planned for 2015. Including one at Big Bear Solar Observatory, for which we will coordinate with NASA program managers.

5. **Publications:**

Allred, Joel C.; Kowalski, Adam F.; Carlsson, Mats, “A Unified Computational Model for Solar and Stellar Flares”, 2015, Ap.J., 809, 104

Battaglia, M, Kleint, L, Krucker, S, Graham, D.: "How important are electron beams in driving chromospheric evaporation in the 2014 March 29 flare?", 2015, ApJ 813, 113

Fleishman, G.D., Xu, Y., Nita, G. N. and Gary, D.E., Validation of the Coronal Thick Target Source Model, 2016, Ap.J., 816, 12

Jing, J., Xu, Y., Lee, J., Nitta, N. V., Liu, C., Park, S.-H., Wiegelmann, T., Wang, H. 2015, Comparison between the eruptive X2.2 flare on 2011 February 15 and confined X3.1 flare on 2014 October 24, RAA, 15, 1537-1546

Kennedy, Michael B.; Milligan, Ryan O.; Allred, Joel C.; Mathioudakis, Mihalis; Keenan, Francis P., “Radiative hydrodynamic modelling and observations of the X-class solar flare on 2011 March 9”, 2015, Ap.J., 578,72

Kleint, L., Heinzel, P., Judge, P., Krucker, S.: "Continuum Enhancements in the Ultraviolet, the Visible, and the Infrared during the X1 flare on 2014 March 29, 2016 ApJ, 816, 88

Kleint, L, Battaglia, M., Reardon, K., Sainz Dalda, A., Young, P.R., Krucker, S. "The Fast Filament Eruption Leading to the X-flare on 2014 March 29", 2015, ApJ 806, 9

Kosovichev, A.G. Sunquakes: Helioseismic Response to Solar Flares, in “Extraterrestrial Seismology”, Cambridge Univ. Press, 2015.

Kowalski, Adam F.; Hawley, S. L.; Carlsson, M.; Allred, J. C.; Uitenbroek, H.; Osten, R. A.; Holman, G. “New Insights into White-Light Flare Emission from Radiative-Hydrodynamic Modeling of a Chromospheric Condensation”, 2015, Solar Physics, 290, 3487

Kuroda, Natsuha; Wang, Haimin and Gary, Dale E., Observation of the 2011-02-15 X2.2 Flare in the Hard X-Ray and Microwave, 2015, Ap.J., 807, 124

Liu, C., Deng, N., Liu, R., Lee, J., Pariat, E., Wiegelmann, T., Liu, Y., Kleint, L., & Wang, H. 2015, A Circular-ribbon Solar Flare Following an Asymmetric Filament Eruption, ApJ Letters, 812, L19(7pp)

Liu, W., P. Heinzel, L. Kleint, J. Kasparova: "Mg II Lines Observed during the X-class Flare on 29 March 2014 by the Interface Region Imaging Spectrograph", 2016, SoPh, in press

Joshi, N.C., Liu, C., Sun, X., Wang, H., Magara, T., & Moon, Y.-J. 2015, The Role of Erupting Sigmoid in Triggering a Flare with Parallel and Large-scale Quasi-circular Ribbons, ApJ, 812, 50(15pp)

Judge, P., Kleint, L., Sainz Dalda, A.: "On helium line polarization during the impulsive phase of an X1 flare", 2015 ApJ, 814, 100

Judge, P.G., Kleint, L., Uitenbroek, H. et al.: "Photon Mean Free Paths, Scattering, and Ever-Increasing Telescope Resolution", 2015, SoPh 290, 979

Petrosian, Vahe' 2015 Particle Acceleration in Solar Flares and Associated CME Shocks, to be submitted to ApJ

Rubio da Costa, F.; Petrosian, V; Liu, W., & Carlsson, M., Combining RADYN and FLARE: modeling the solar atmosphere during solar flares, 2015a, ApJ, 813, 133

Rubio da Costa, F.; Kleint, L.; Sainz-Dalda, A.; Petrosian, V & Liu, W., Solar Flare Chromospheric Line Emission: Comparison Between IBIS Observations and Radiative Transfer Hydrodynamic Simulations, 2015b, ApJ, 804, 562

Rubio da Costa, F.; L. Kleint; A. Sainz Dalda; V. Petrosian; W. Liu, Radiative hydrodynamic modeling and observations of the X-class solar flare on 2014 March 2, 2016, to be submitted to ApJ

Sadykov, V.M., S. Vargas Dominguez, A.G. Kosovichev, I.N. Sharykin, A.B. Struminsky, and I. Zimovets, Properties of Chromospheric Evaporation and Plasma Dynamics of a Solar Flare from Iris. The Astrophysical Journal, 2015. 805: p. 167.

Sharykin, I.N. and A.G. Kosovichev, Dynamics of Electric Currents, Magnetic Field Topology, and Helioseismic Response of a Solar Flare. The Astrophysical Journal, 2015. 808: p. 72.
Sharykin, I.N., A.G. Kosovichev, and I.V. Zimovets, Energy Release and Initiation of a Sunquake in a C-class Flare. The Astrophysical Journal, 2015. 807: p. 102.

Vargas Domínguez, S., V. Sadykov, A. Kosovichev, I. Sharykin, A. Struminsky, and I. Zimovets, NST and IRIS multi-wavelength observations of an M1.0 class solar flare. IAU General Assembly, 2015. 22: p. 57574.

Wang, H. & Liu, C. 2015, Structure and Evolution of Magnetic Fields Associated with Solar Eruptions (Invited Review), RAA, 15, 145-174

Wang, H., Cao W., Liu, C., Xu Y., Liu R., Zeng Z., Chae J., & Ji H. 2015, Witnessing magnetic twist with high-resolution observation from the 1.6-m New Solar Telescope, Nature Communication, 6, 7008